

Photorefractivity in Nematic Liquid Crystals Using a Donor–Acceptor Dyad with a Low-Lying Excited Singlet State for Charge Generation

Michael J. Fuller and Michael R. Wasielewski*

Department of Chemistry and Center for Nanofabrication and Molecular Self-Assembly,
Northwestern University, Evanston, Illinois 60208-3113

Received: April 25, 2001

The photorefractive effect was observed in room-temperature nematic liquid crystal composites consisting of a eutectic mixture of 65% 4'-(*n*-pentyl)-4-cyanobiphenyl and 35% 4'-(*n*-octyloxy)-4-cyanobiphenyl doped with a donor–acceptor dyad in which 9-(*N*-pyrrolidiny)perylene-3,4-dicarboximide is directly linked to 1,8:4,5-naphthalenetetracarboxydiimide. This dyad has a broad, intense absorption band that extends from 500 to 750 nm. Measurements of two-beam asymmetric energy exchange (beam-coupling) and the diffraction efficiency of the refractive index grating produced in these liquid crystal thin films were carried out. A comparison is made between the covalent donor–acceptor dyad and the corresponding noncovalent donor–acceptor pair. In each case the covalent dyad outperforms the noncovalent donor–acceptor pair. The results show that aminoaryleneimides are promising new charge donating chromophores that are capable of extending photorefractive performance of nematic liquid crystal composites into the near-infrared region of the spectrum.

Introduction

Organic photorefractive materials display significant potential for use in optical data storage, image amplification, phase conjugate mirrors, and dynamic holography.^{1–7} Films of aligned nematic liquid crystals (LCs) doped with chromophores capable of charge separation and transport over macroscopic distances exhibit significant photorefractive effects.^{8–12} Two coherent cw laser beams that cross within an aligned LC sample produce a light intensity grating in the material. Absorption of a small fraction of the light by a chromophoric electron donor or acceptor within the illuminated regions of the grating results in photoinduced electron transfer leading to the formation of radical ion pairs. A difference in diffusion coefficients for the two oppositely charged ions coupled with a mechanism for trapping each of the ions separately in the light and dark regions of the grating results in a space charge field. This periodic electric field produces a refractive index grating in the LC due principally to the quadratic electrooptic effect. The refractive index grating and the light intensity grating within the material are phase shifted relative to one another, which results in asymmetric energy exchange (two-beam coupling) between the two laser beams that produce the grating. Two-beam coupling is diagnostic for the photorefractive effect. In general, the wavelength of light that produces the charges which generate the space charge field determines the wavelength at which a particular photorefractive material can be used for optical image processing and storage. Therefore, it is important to develop photorefractive materials that are active at near-infrared wavelengths because these wavelengths are of special interest to optical communications technology.^{13,14}

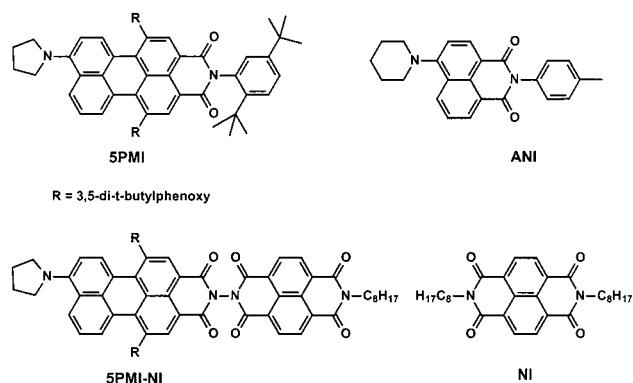
Toward this goal we have developed a push–pull perylene, **5PMI**, which acts as good electron donor, and can be covalently attached to electron acceptors. This donor is easy to oxidize, displays a high optical extinction coefficient, and absorbs significantly to the red of the corresponding push–pull 4-(*N*-

piperidiny)naphthalene-1,8-dicarboximide (**ANI**), which we have used previously in charge generation and transport dopants in photorefractive LC composites.¹⁵

Charge generation reactions that use intramolecular electron transfer within a covalently linked donor–acceptor pair have been studied both in doped and functionalized photorefractive polymers.^{16,17} Donor–acceptor dyad dopants, D–A in photorefractive LC composites undergo quantitative intramolecular charge separation to yield D⁺–A[−]. These ion pairs recombine much more slowly in the nematic LC, due to control of the recombination rate by the relatively slow reorientation of the LC dipole.¹⁸ When the long-lived D⁺–A[−] pairs encounter a neutral D–A pair, intermolecular electron-transfer yields D⁺–A and D–A[−] pairs, which separate with different diffusion coefficients. Covalent dyads offer the distinct advantage that their quantum efficiencies of charge generation are close to unity. It has been shown that this high yield of charges translates directly into enhanced photorefractivity.¹⁵

Experimental Methods

The syntheses of **5PMI**, **NI**, and **5PMI-NI** are presented in the Supporting Information. Their structures, as well as the structure of **ANI**, are shown below.



* To whom correspondence should be addressed. E-mail: wasielew@chem.northwestern.edu.

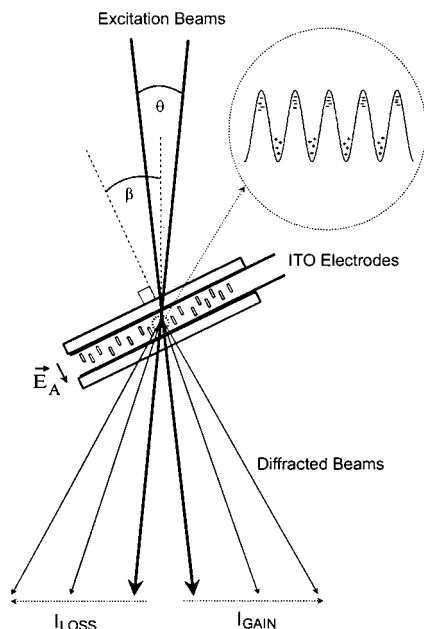


Figure 1. A schematic of the experimental geometry for two-beam coupling and diffraction efficiency measurements is illustrated. The laser beams are p-polarized in the plane of the page. E_A is the applied electric field.

Electrochemical measurements were performed with a CH Instruments model 660 system using Pt working and counter electrodes as well as a Ag/AgCl reference electrode. Potentials were measured in benzonitrile containing 0.1 M tetra-*n*-butylammonium perchlorate. Ferrocene was used as an internal reference. The nematic LC solvent used in these studies is a mixture of 35% 4'-(*n*-octyloxy)-4-cyanobiphenyl (8OCB) (Aldrich) and 65% 4'-(*n*-pentyl)-4-cyanobiphenyl (5CB) (Aldrich) by weight. This specific LC mixture was chosen because the temperature range of its nematic phase is broad, and its viscosity at room temperature is lower than that of 5CB alone. Indium tin oxide (ITO)-coated glass slides were functionalized with the surfactant octadecyltrichlorosilane to induce homeotropic alignment of the LC mixture. The path length of the cells was 26 μm thick, as determined by a cellulose triacetate spacer. The doped 5CB/8OCB mixture was introduced into the cell by capillary action, and alignment of the LC mixture occurred in a few minutes yielding cells of high optical quality.

Two-beam coupling and diffraction efficiency measurements were obtained using the experimental geometry shown in Figure 1, where two coherent beams of equal energy from a tunable Ar^+ laser operating at 514.5 nm cross in the sample cell, the normal of which is tilted $\beta = 30^\circ$ relative to the bisector of the two intersecting laser beams. The crossing angle $\theta = 0.53^\circ$ fixes the grating spacing at $\Lambda = 37 \mu\text{m}$, which was employed for all the measurements described here. As the diffraction pattern is present only when a small voltage ($< 2 \text{ V}$) is applied to the cell and p-polarized laser beams are used, the grating is an orientational photorefractive grating and not a thermal or absorption grating.^{5,8,11,19} Beam coupling ratios rather than gain values are reported because the photorefractive gain is poorly defined for a thin, Raman-Nath grating.²⁰ Photoconductivity measurements were made by illuminating the entire cell, which has approximately a 4 cm^2 surface area with a 50 mW, 514 nm Ar^+ laser beam. The cell was biased at voltages comparable to those used for the two-beam coupling and diffraction efficiency measurements. Both photoconductivity and dark conductivity measurements were made with a Keithley model 485 picoammeter.

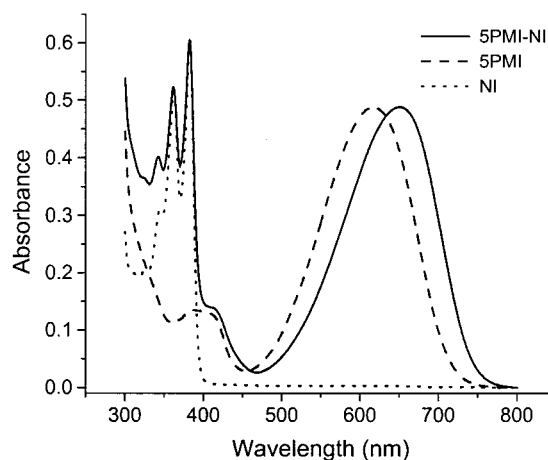


Figure 2. Ground-state absorption spectra of **5PMI-NI**, **5PMI**, and **NI** in benzonitrile.

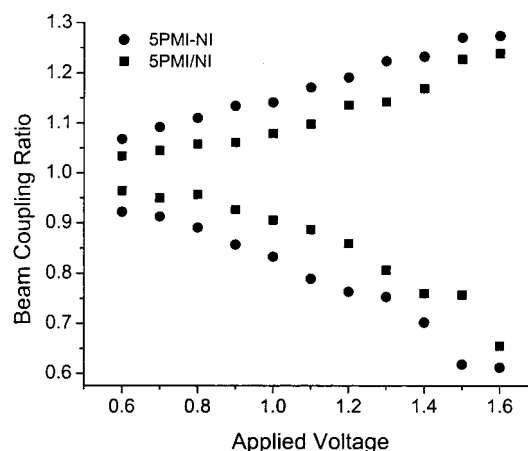


Figure 3. The asymmetric two-beam coupling data for **5PMI-NI** (8.0×10^{-4}) and for **PMI** (1.0×10^{-3})/**NI** (3.0×10^{-3}) in a 5CB/8OCB mixture (as calculated by the ratio of intensity of the beam that gains (loses) intensity relative to its intensity incident upon the sample) is illustrated.

Results and Discussion

The ground-state absorption spectrum of each molecule in benzonitrile is illustrated in Figure 2. The broad absorption band of **5PMI-NI** extends from 500 to 750 nm with a maximum at 650 nm, while its fluorescence spectrum (not shown) has a maximum at 755 nm. The energy of the lowest excited singlet state of **5PMI-NI** E_s , calculated from the average of the energies of the absorption and fluorescence maxima, is 1.77 eV. The oxidation potential E_{OX}^D of the **5PMI** donor is 0.61 V vs SCE, which is significantly lower than the corresponding 1.2 V oxidation potential for the **ANI** donor previously studied as a dopant in photorefractive LC composites.¹⁵ The reduction potential E_{RED}^A of **NI** is -0.53 V , so that the free energy of the reaction $^1\text{5PMI-NI} \rightarrow \text{5PMI}^+-\text{NI}^-$ in the polar LC is approximately $\Delta G_{\text{CS}} = E_{\text{OX}}^D - E_{\text{RED}}^A - E_s = -0.63 \text{ eV}$.

Figure 3 compares the beam coupling ratio data for **5PMI-NI** and **5PMI/NI** mixtures. The **5PMI-NI** donor-acceptor dyad exhibits higher beam coupling ratios, and therefore enhanced photorefractivity, at all applied voltages compared to the **5PMI/NI** mixtures. It is also noteworthy that the data presented in Figure 3 show that lower concentrations of **5PMI-NI** are necessary to achieve efficient asymmetric energy exchange between interfering beams than **5PMI/NI** mixtures.

Diffraction efficiency η measurements were carried out to compare the performance of the two composites. The diffraction

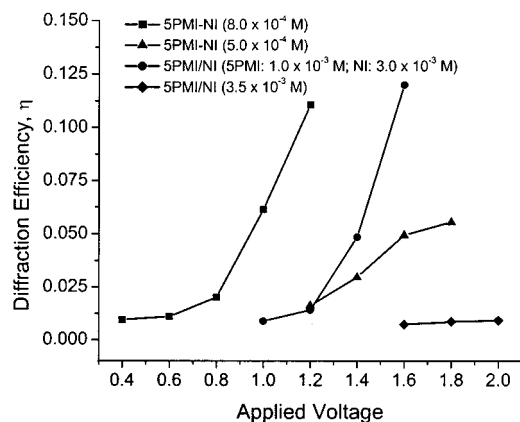


Figure 4. The first-order diffraction efficiency (η) of the photorefractive grating for a variety of LC composites is illustrated.

efficiency in these thin (Raman–Nath) gratings is calculated as the ratio of the intensity of the first diffracted beam to the intensity of one of the writing beams incident upon the sample. Several concentrations of both **5PMI-NI** and **5PMI/Ni** were examined, and Figure 4 plots the diffraction efficiency η against applied voltage. It is apparent that the composite achieving the best diffraction efficiency at the lowest voltage is the one doped with **5PMI-NI** (8.0×10^{-4} M). The composite containing **5PMI** (1.0×10^{-3} M)/**Ni** (3.0×10^{-3} M) requires an additional 0.4 V applied to the film to achieve a comparable diffraction efficiency. Figure 4 also shows that the diffraction efficiency of the composite using a **5PMI/Ni** mixture with a 3x molar excess of **Ni** is better than that of one doped with equimolar amounts of **5PMI** and **Ni**. This behavior is consistent with the expected increased efficiency of the reaction: ${}^1\text{5PMI} + \text{Ni} \rightarrow \text{5PMI}^+ + \text{Ni}^-$, when higher concentrations of either reactant are present.

The diffraction efficiency η of a Raman–Nath orientational grating is given by⁸

$$\eta = \left(\frac{Lmk_B T}{\lambda n_e K q e} \right) \left(\frac{E_A \epsilon_s \epsilon_\infty \sin \beta}{1 + \frac{\epsilon_\infty E_A^2}{2\pi K q^2}} \right) \left(\frac{\sigma_{ph}}{\sigma_{ph} + \sigma_d} \right) \nu^2 \quad (1)$$

$$\text{where} \quad \nu = \frac{D^+ - D^-}{D^+ + D^-} \quad (2)$$

D^+ and D^- are the diffusion constants for the cations and anions, respectively; L is the thickness of the sample, m is the modulation index, which equals 1 if equal intensity beams generate the grating; k_B is the Boltzmann constant, T is the temperature, q is the wavevector of the grating, λ is the wavelength; n_e is the index of refraction along the extraordinary axis; K is the single constant approximation of the Frank elastic constant;⁸ e is the electronic charge; E_A is the voltage applied to the cell; ϵ_s is the average static dielectric constant of the LC; ϵ_∞ is the high-frequency dielectric constant; σ_{ph} is the photoconductivity; and σ_d is the dark conductivity.

It is clear from eq 1 that two important factors that determine the diffraction efficiency are the difference between the photoconductivity and the dark conductivity and the difference between the diffusion coefficients of the cations and anions. The data in Figure 5 show that the dark conductivity of the sample rises significantly when the applied voltage is greater than about 1.5 V. This increase in dark conductivity with increasing applied voltage is most likely due to faradaic redox

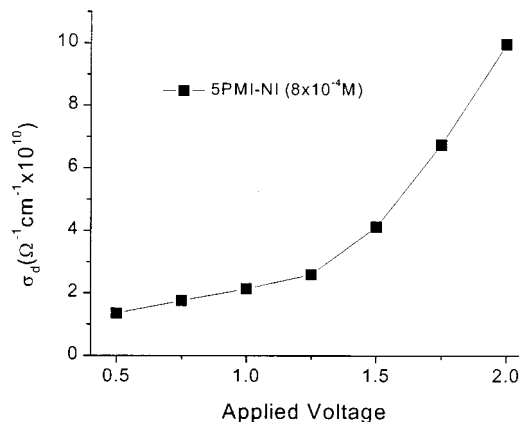


Figure 5. Dark conductivity as a function of applied voltage for **5PMI-NI** (8.0×10^{-4}) in a 5CB/8OCB mixture.

processes involving oxidation of the donor and/or reduction of the acceptor molecules at the ITO electrodes. The rates of these redox processes are retarded by the octadecylsiloxane layer on the ITO, but these thin layers do not completely inhibit the redox chemistry. By comparison the photoconductivity at low voltages is about $10^{-11} \text{ ohm}^{-1} \text{ cm}^{-1}$, and is weakly dependent on voltage for voltages < 2 V. The data in Figure 5 suggest that voltages below 1.5 V are necessary to maintain a reasonable ratio of $\sigma_{ph}/(\sigma_{ph} + \sigma_d)$. Using the values $K = 7 \times 10^{-7} \text{ dyne}$,²¹ $n_e = 1.5$, $\epsilon_\infty = 2.25$, $\epsilon_s = 10.5$, $T = 298 \text{ K}$, $L = 26 \text{ } \mu\text{m}$, $m = 1$, $\lambda = 514 \text{ nm}$, $q = 3.7 \times 10^3 \text{ cm}^{-1}$, $E_A = 1.2 \text{ V}$, $\sigma_{ph} = 10^{-11} \text{ ohm}^{-1} \text{ cm}^{-1}$, and $\sigma_d = 10^{-10} \text{ ohm}^{-1} \text{ cm}^{-1}$, along with the measured value of $\eta = 0.11$ for the composite containing **5PMI-NI** at 1.2 V, eq 1 yields $\nu = 0.25$. This value is comparable to $\nu = 0.29$ obtained for the corresponding **ANI-Ni** system at 1.5 V reported earlier.¹⁵ Since the diffraction efficiency for the **5PMI/Ni** sample is 0.013 at 1.2 V, eq 1 yields $\nu = 0.08$. Given the definition of ν in eq 2, the larger value of ν for **5PMI-Ni** shows that the difference in diffusion coefficients between the **5PMI}^+**-**Ni** and **5PMI-Ni}^-** ions is greater than that between **5PMI}^+** and **Ni}^-**. This results in a more efficient photorefractive grating using the **5PMI-Ni** dyad.

Conclusions

We have demonstrated that an aminoaryleneimide with extended conjugation, **5PMI**, which possesses a low energy absorption band extending into the near-infrared region of the spectrum, exhibits significant photorefractive effects in nematic LC composites. Moreover, using a covalently linked **5PMI-Ni** donor–acceptor pair for charge generation rather than the corresponding noncovalent mixture of **5PMI** and **Ni** significantly improves performance. This work indicates that molecular designs based on extended aminoaryleneimides should allow us to produce new charge generation materials for photorefractive LC composites to access the near-infrared spectral region.

Acknowledgment. We gratefully acknowledge support from the Office of Naval Research under Grant N00014-99-1-0411.

Supporting Information Available: Syntheses of **5PMI**, **Ni**, and **5PMI-Ni**. This material is available free of charge via the Internet at <http://pubs.acs.org>.

References and Notes

- (1) Feinberg, J. *Phys. Today* **1988**, *41*, 46.
- (2) Dinu, M.; Nakagawa, K.; Melloch, M. R.; Weiner, A. M.; Nolte, D. D. *J. Opt. Soc. Am. B* **2000**, *17*, 1313.

- (3) Goonesekera, A.; Wright, D.; Moerner, W. E. *Appl. Phys. Lett.* **2000**, *76*, 3358.
- (4) Shamir, J.; Caulfield, H. J.; Hendrickson, B. M. *Appl. Opt.* **1988**, *27*, 2912.
- (5) Wiederrecht, G. P.; Yoon, B. A.; Wasielewski, M. R. *Adv. Mater.* **1996**, *8*, 535–539.
- (6) Feinberg, J.; Hellwarth, R. W. *Opt. Lett.* **1980**, *5*, 519.
- (7) Nolte, D. D.; Olson, D. H.; Doran, G. E.; Knox, W. H.; Glass, A. M. *J. Opt. Soc. Am. B* **1990**, *7*, 2217.
- (8) Rudenko, E. V.; Sukhov, A. V. *JETP Lett.* **1994**, *59*, 142.
- (9) Zhang, J.; Ostroverkhov, V.; Singer, K. D.; Reshetnyak, V.; Reznikov, Y. *Opt. Lett.* **2000**, *25*, 414.
- (10) Khoo, I. C.; Slussarenko, S.; Guenther, B. D.; Shih, M. Y.; Chen, P.; Wood, W. V. *Opt. Lett.* **1998**, *23*, 253.
- (11) Wiederrecht, G. P.; Yoon, B. A.; Wasielewski, M. R. *Science* **1995**, *270*, 1794–1797.
- (12) Wiederrecht, G. P.; Niemczyk, M. P.; Svec, W. A.; Wasielewski, M. R. *Chem. Mater.* **1999**, *11*, 1409.
- (13) Day, D.; Gu, M.; Smallridge, A. *Opt. Lett.* **1999**, *24*, 948.
- (14) Van Steenwinckel, D.; Engels, C.; Gubbelsmans, E.; Hendrickx, E.; Samyn, C.; Persoons, A. *Macromolecules* **2000**, *33*, 4074.
- (15) Wiederrecht, G. P.; Yoon, B. A.; Svec, W. A.; Wasielewski, M. R. *J. Am. Chem. Soc.* **1997**, *119*, 3358–3364.
- (16) Yu, L.; Chan, W. K.; Peng, Z.; Gharavi, A. *Acc. Chem. Res.* **1996**, *29*, 13.
- (17) Marder, S.; Kippelen, B.; Jen, A. K.; Peyghambarian, N. *Nature* **1997**, *388*, 845.
- (18) Wiederrecht, G. P.; Svec, W. A.; Wasielewski, M. R. *J. Phys. Chem. B* **1999**, *103*, 1386–1389.
- (19) Khoo, I. C.; Li, H.; Liang, Y. *Opt. Lett.* **1994**, *19*, 1723–1725.
- (20) Moerner, W. E.; Grunnet-Jepsen, A.; Thompson, C. L. *Annu. Rev. Mater. Sci.* **1997**, *27*, 585–623.
- (21) Khoo, I. C. *Liquid Crystals: Physical Properties and Nonlinear Optical Phenomena*; Wiley: New York, 1995.